3 Calcium Dynamics

Intracellular calcium Ca^{2+} is important in a number of physiological systems, for instance skeletal and cardiac muscle contraction, the regulation of the exocrine and endocrine systems, cell motility and exocytosis. More than 99% of Ca^{2+} in the body is stored in skeletal bones, from where it is released by hormonal stimulation to maintain an extracellular Ca^{2+} concentration of around 10^{-3}M (1M = 1 molar = 1 mole/litre). In contrast, intracellular cytosolic Ca^{2+} concentrations are low, around 10^{-7}M, and therefore control mechanisms must exist to

(i) keep intracellular levels low,

(ii) enable rapid release when required.

In addition, under certain circumstances, for instance hormonal stimulation, oscillations in Ca^{2+} concentrations can occur.

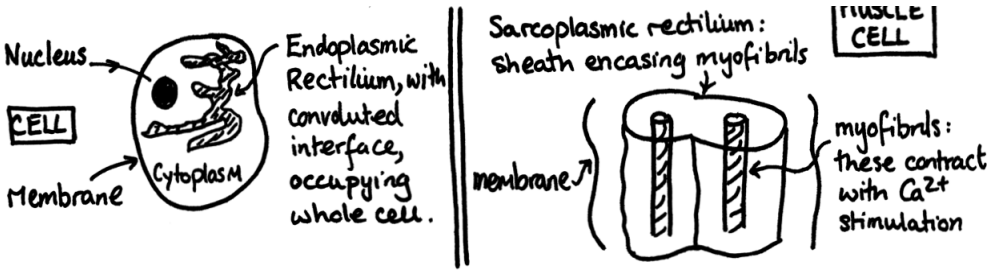

Figure 1: Endoplasmic reticulum and sarcoplasmic reticulum

At the cellular level, high levels of calcium ($\sim 10^{-3}$M) are also present in the internal cell compartments, for instance the stores of the endomembrane system, generally denoted the *endoplasmic reticulum* (ER) though with a specialised form, the *sarcoplasmic reticulum* (SR), in skeletal and cardiac muscle.
Calcium release from the intracellular stores occurs through IP_3 (inositol (1,4,5)-triphosphate) receptors and Ryanodine (RyR) receptors and both modes of release can be present in the same cell, for both contractile and non-contractile cells.

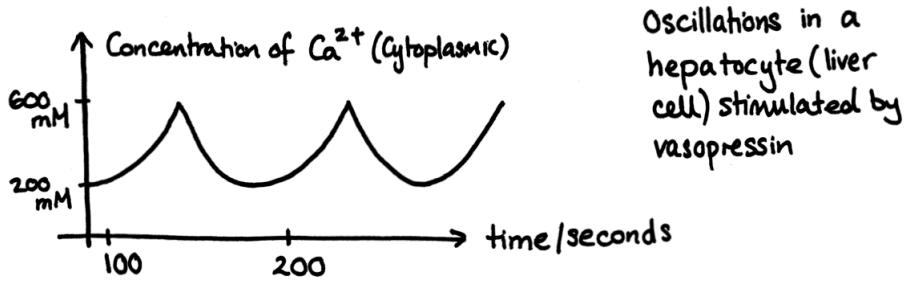

Figure 2: Oscillations in a hepatocyte (liver cell) stimulated by vasopressin.

Oscillations occur when cells are stimulated by neurotransmitters or hormones and manifest in a limited range of stimulation intensity and are spiky with frequency increases on intensifying the stimulation.

3.1 The Two Pool Model

Mechanisms

Calcium release from the intracellular stores can be initiated via a hormone induced release of IP_3 (inositol (1,4,5)-triphosphate), which diffuses to IP_3 receptors on the store membranes, opening gates in turn allowing the release of Ca^{2+}.

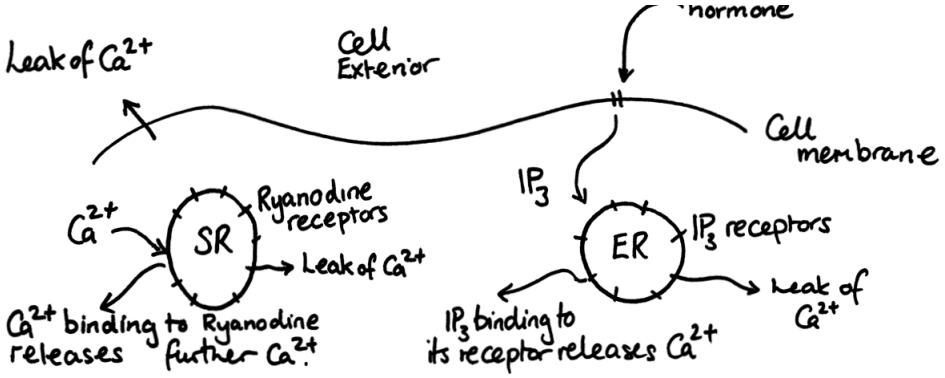

Figure 3: Schematic of two pool model.

Ryanodine receptors on the store membrane are associated with Ca^{2+} induced Ca^{2+} release (CICR), whereby uptake of calcium by Ryanodine induces a release of calcium from the store, with a net effect of releasing calcium into the cytosol.

The model

Let

- c denote the concentration of Ca^{2+} in the cytosol
- c_s denote the concentration of Ca^{2+} in the Ca^{2+} sensitive store.

We further assume that Ca^{2+} is constant in the IP_3 sensitive store, so that the stimulus produces a constant release rate of Ca^{2+}. In addition, there are linear leakages of ions from the store, the constant terms from which can be combined with IP_3 release rate, to give an effective release rate. In terms of the fluxes J_+, J_- for the Ryanodine Ca^{2+} uptake and the Ca^{2+} induced Ca^{2+} release, the equations are therefore:

$$\frac{dc}{dt} = \underbrace{r}_{\text{release from ER}} \underbrace{- kc}_{\text{leak to cell exterior}} - \Big[\underbrace{J_+}_{\text{uptake by Ryanodine}} - \underbrace{J_-}_{\substack{Ca^{2+}\text{ induced} \\ Ca^{2+}\text{ release flux}}} \underbrace{- k_s c_s}_{\substack{\text{leaks} \\ \text{from} \\ \text{stores}}}\Big]$$

$$\frac{dc_s}{dt} = J_+ - J_- - k_s c_s$$

We take Hill forms for the fluxes:

$$J_+ = \frac{V_1 c^n}{K_1^n + c^n}, \qquad J_- = \frac{V_2 c_s^m}{K_2^m + c_s^m}\frac{c^p}{K_3^p + c^p},$$

where $m,\ p > n$ are positive integers and $V_1,\ V_2,\ K_1,\ K_2,\ K_3$ are positive constants. Non-dimensionalising with

$$c = K_1 u, \quad t = \frac{\tau}{k}, \quad c_s = K_2 v,$$

yields:

$$K_1 k\frac{du}{d\tau} = r - kK_1 u - \left(\frac{V_1 u^n}{1+u^n} - \frac{V_2 v^m}{1+v^m}\frac{u^p}{\alpha^p + u^p} - k_s K_2 v\right)$$

and hence

$$\frac{du}{d\tau} = \mu - u - \frac{\gamma}{\epsilon} f(u,v),$$

with

$$\alpha = \frac{K_3}{K_1}, \quad \mu = \frac{r}{kK_1}, \quad \beta = \frac{V_1}{V_2}, \quad \delta = \frac{k_s K_2}{V_2}, \quad \gamma = \frac{K_2}{K_1}, \quad \epsilon = \frac{kK_2}{V_2},$$

$$f(u,v) = \beta\left(\frac{u^n}{1+u^n}\right) - \left(\frac{v^m}{1+v^m}\right)\left(\frac{u^p}{\alpha^p + u^p}\right) - \delta v.$$

Similarly

$$K_2 k\frac{dv}{d\tau} = V_2 f(u,v),$$

and hence

$$\frac{dv}{d\tau} = \frac{1}{\epsilon} f(u,v).$$

Parameter Values
With

$$k = 10\text{s}^{-1},\ K_1 = 1\mu\text{M},\ K_2 = 2\mu\text{M},\ K_3 = 0.9\mu\text{M},\ V_1 = 65\mu\text{Ms}^{-1},\ V_2 = 500\mu\text{Ms}^{-1},$$

$$k_s = 1\text{s}^{-1},\ p = 4,\ n = 2,\ m = 2,$$

we have

$$\alpha = 0.9,\ \beta = 0.13,\ \gamma = 2,\ \delta = 0.004,\ \epsilon = 0.04, \mu = \frac{r}{10} \sim 1 \text{ if } r = 10\mu\text{Ms}^{-1}.$$

Below, it will be useful to treat μ as a control parameter.

3.1.1 Phase Plane Analysis

The equations are

$$\frac{du}{d\tau} = \mu - u - \frac{\gamma}{\epsilon} f(u,v) = \mu - u - \gamma \frac{dv}{d\tau}, \qquad \epsilon \frac{dv}{d\tau} = f(u,v),$$

$$f(u,v) = \beta \left(\frac{u^n}{1+u^n} \right) - \left(\frac{v^m}{1+v^m} \right) \left(\frac{u^p}{\alpha^p + u^p} \right) - \delta v.$$

As $\epsilon \ll 1$, we have fast and slow dynamics.

Fast Dynamics Unless $f(u,v) \approx 0$ the variable v will evolve on a fast timescale. Let

$$T = \tau/\epsilon$$

be a fast time variable: we have

$$\frac{dv}{dT} = f(u,v), \qquad \frac{du}{dT} + \gamma \frac{dv}{dT} = 0$$

at leading order, and hence $u + \gamma v$ is approximately constant.

Slow Dynamics When v is not changing rapidly, we work with the slow time variable τ, and we have at leading order in ϵ that

$$f(u,v) = 0.$$

We can invoke the implicit function theorem to write this constraint in the form $v = g(u)$, for some function $g(u)$, which we do not have an explicit form for at present. Then

$$\frac{du}{d\tau} + \gamma \frac{dv}{d\tau} = (1 + \gamma g'(u)) \frac{du}{d\tau} = \mu - u.$$

Phase Plane
First we consider the v nullcline $f(u,v) = 0$ and determine $v = g(u)$. We define the following functions

$$\begin{aligned} L(v) &= \frac{v^m}{1+v^m}, \\ J(u) &= \beta \left(\frac{u^n}{1+u^n} \right), \\ K(u) &= \frac{u^p}{\alpha^p + u^p}, \end{aligned}$$

where $m = 2, n = 2, p = 4, \beta = 0.13$ and $\alpha = 0.9$.
Neglecting $\delta \ll 1$ in the first instance gives

$$f(u,v) = J(u) - L(v)K(u),$$

and so $f = 0$ corresponds to

$$L(v) = \frac{J(u)}{K(u)}. \tag{1}$$

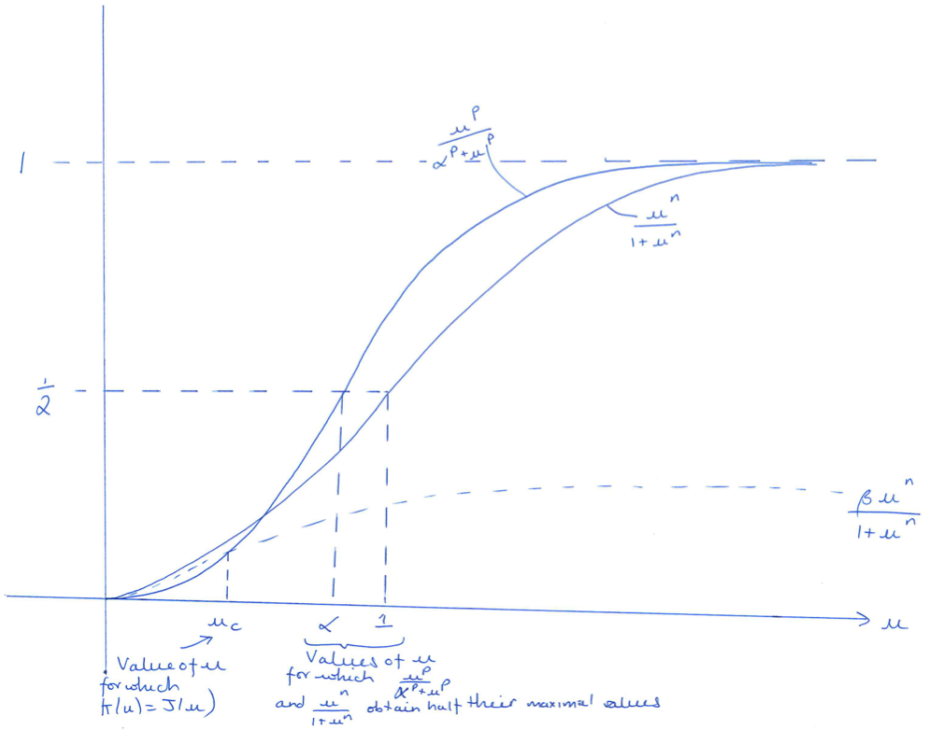

Figure 4: Graphs of $J(u)$ and $K(u)$.

We now consider the forms of $J(u)$ and $K(u)$ (see figure (4)). We note that

$$\frac{u^n}{1+u^n} \sim u^n \text{ as } u \to 0, \quad \frac{u^n}{1+u^n} \sim 1 - \frac{1}{u^n} \text{ as } u \to \infty. \tag{2}$$

From these curves, we can deduce the form of

$$R(u) = \frac{J(u)}{K(u)}, \tag{3}$$

noting that $R = 1$ and $u = u_c$ (see figure (5) for a plot of $R(u) = J(u)/K(u)$).
Now since we have that $v^m/(1+v^m) \leq 1$, the approximation that $L(v) = R(u)$ cannot hold for $R > 1$, *i.e.* the assumption that we can neglect the term involving δ is the expression for $f(u, v)$ breaks down for small u. In fact, the δ term is significant when either $\delta v \sim O(1)$ (*i.e.* v is large) or $J(u), K(u) \sim O(\delta)$ (*i.e.* u is small).

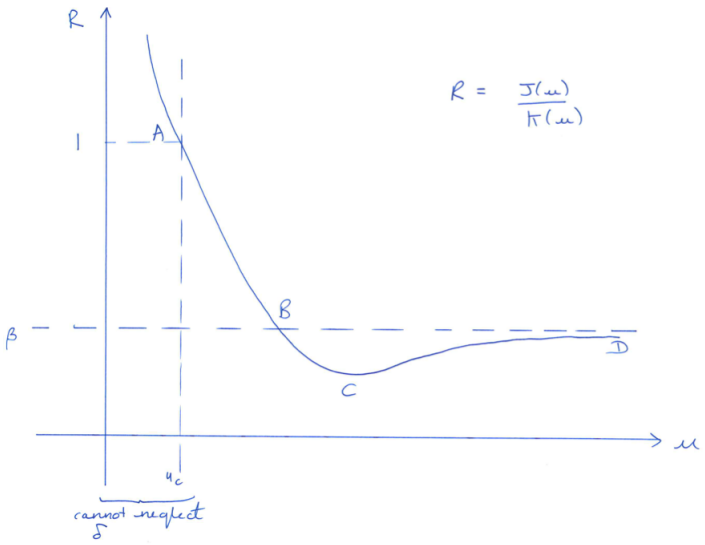

Figure 5: Graph of $R = J(u)/K(u)$.

Figure (5) is a plot of $L(v) = v^m/(1+v^m)$ $(m = 2)$ versus u. However, we are seeking to plot v versus u. We note that $L(v)$ is monotonically increasing (see figure (6)), and that $L(v) = v^2/(1+v^2) < v$. Thus, so far the nullcline is given by figure 7 (where we note that v_β is such that $L(v_\beta) = \beta$).

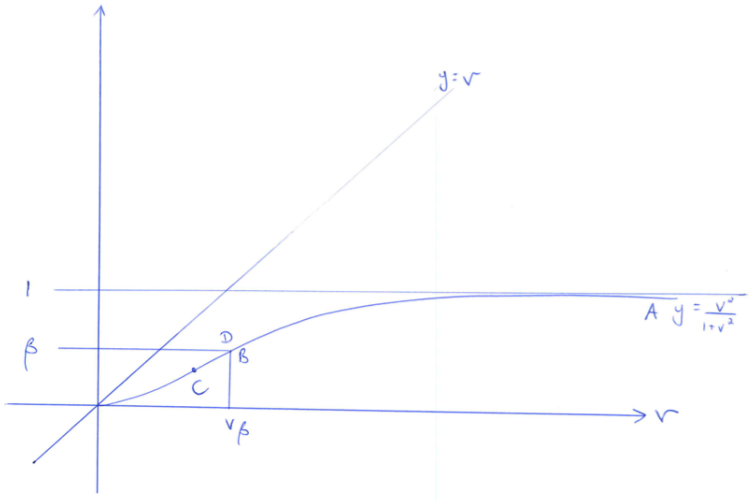

Figure 6: Graph of $L(v)$ versus v.

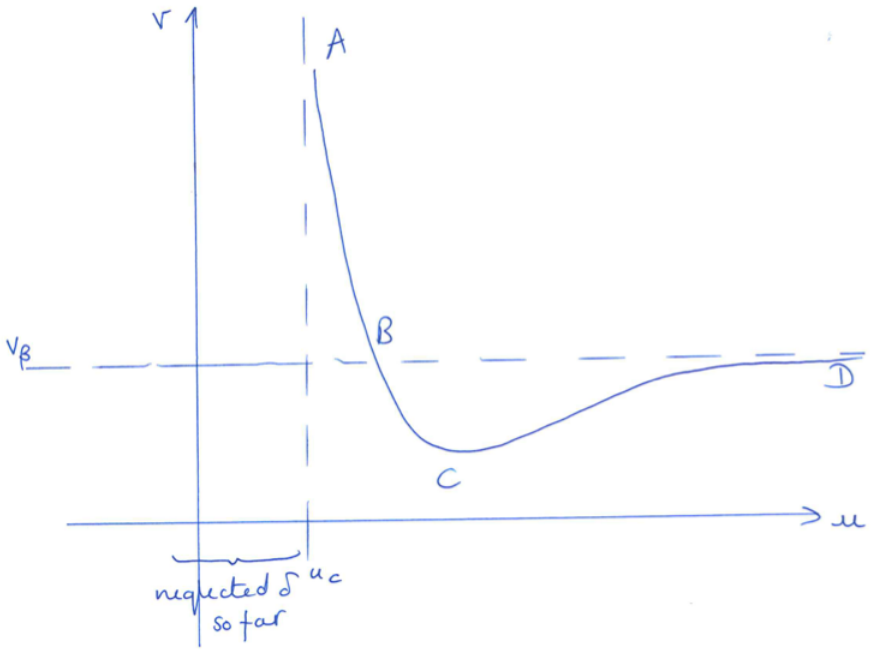

Figure 7: Approximation to the nullcline when terms of $O(\delta)$ are neglected.

When $v \to \infty$, the term δv becomes important again. The nullcline $f(u, v) = 0$ is then given by

$$J(u) - L(v)K(u) - \delta v = 0. \tag{4}$$

Now, if v is large, $L(v) \approx 1$ and hence (4) gives that

$$v \approx \frac{1}{\delta}(J(u) - K(u)), \tag{5}$$

and we note (verify) that this has a turning point for $u < u_c$. We also note that the righthand side of (5) is zero at $u = u_c$. For u small, we can also neglect the $K(u)$ term (since $p > n$) so that

$$v \approx \frac{1}{\delta}\frac{\beta u^n}{1 + u^n}. \tag{6}$$

The approximation to the nullcline is now shown in figure 8.
To piece the curves together (which are each approximations) we consider an overlap region where $v \gg 1$ and $u \approx u_c$. Starting again from

$$f(u, v) = J(u) - K(u)L(v) - \delta v = 0, \tag{7}$$

we expand for v large, u close to u_c as follows

$$J(u_c) + (u - u_c)J'(u_c) + \cdots - (K(u_c) + (u - u_c)K'(u_c) + \cdots)\left(1 - \frac{1}{v^m} + \cdots\right) - \delta v = 0. \tag{8}$$

Now $J(u_c) = K(u_c)$ and we note that $K'(u_c) > J'(u_c)$ and so we have that

$$u - u_c \approx \frac{1}{K'(u_c) - J'(u_c)}\left(\frac{K(u_c)}{v^m} - \delta v\right), \tag{9}$$

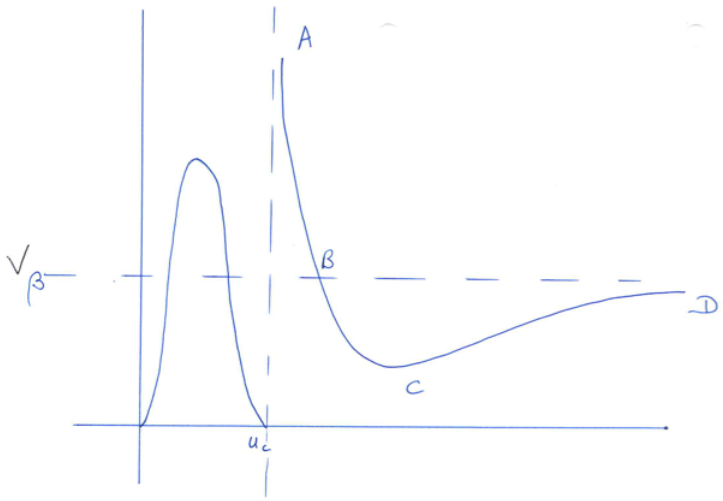

Figure 8: Approximation to the nullcline

so that in the overlap region we have

$$v \sim \frac{1}{\delta^{1/(m+1)}}, \; u - u_c \sim \delta^{m/(m+1)}. \tag{10}$$

Graphs of v versus u in this region are shown in figure 9.
Putting all this information together, the nullcline corresponding to $f(u, v) = 0$, given by $v = g(u)$, is shown in figure 10.

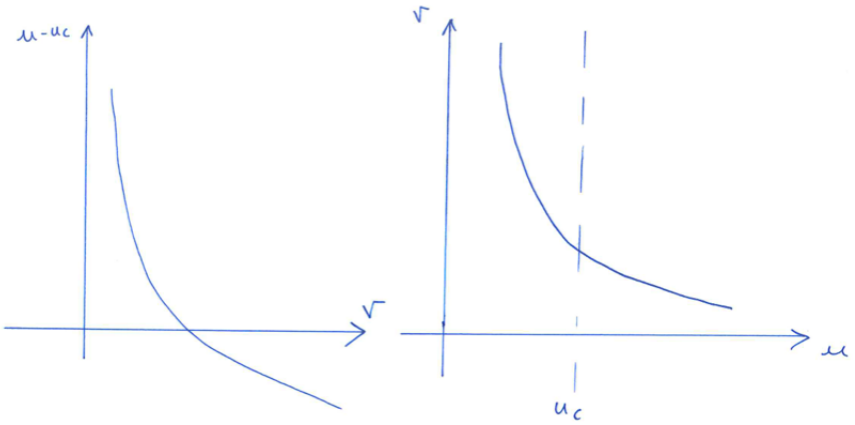

Figure 9: Approximation to the nullcline for v large, u close to u_c.

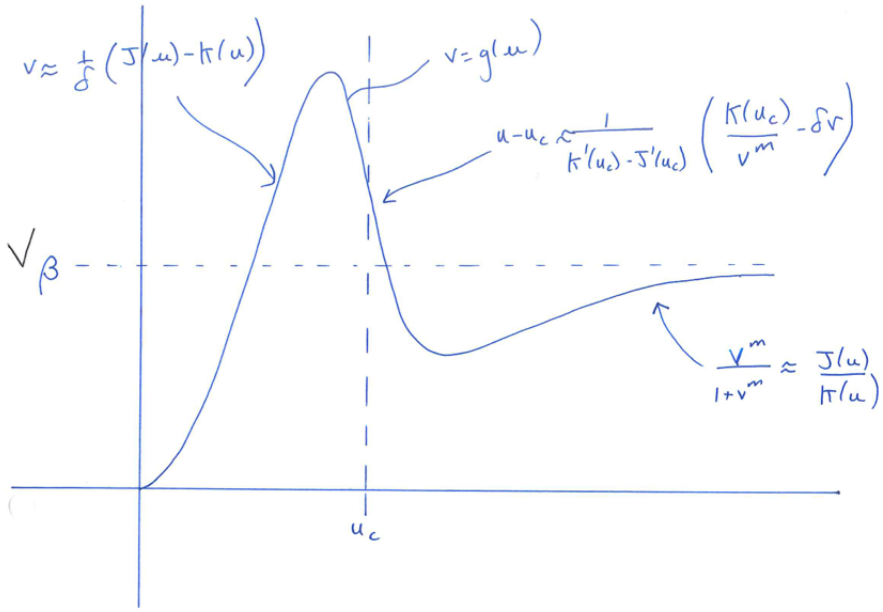

Figure 10: Nullcline corresponding to $f(u, v) = 0$.

We now define various points on the curve, In particular, we define $\mu_\pm$ to be those values of u where

$$g'(\mu_\pm) = -\frac{1}{\gamma}. \tag{11}$$

This is important as on the fast timescale (to leading order) we have that $u + \gamma v$ is approximately constant. The slope of these curves is $-1/\gamma$. See figure 11.

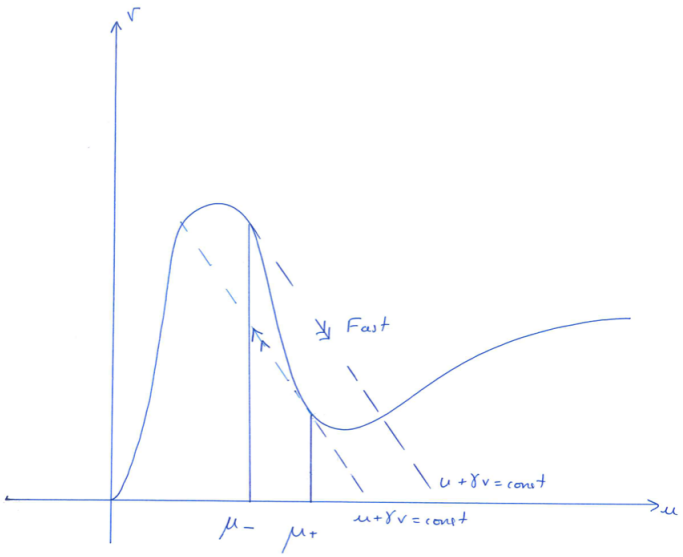

Figure 11: Determining $\mu_\pm$.

We are now in position to analyse the dynamics of the system using phase-plane analysis. We reiterate the governing equations are

$$\frac{d}{d\tau}(u+\gamma v) = \mu - u \tag{12}$$

$$\frac{dv}{d\tau} = \frac{1}{\epsilon} f(u,v). \tag{13}$$

The equilibrium point corresponds to $f(u,v)=0$, $u=\mu$. We start by considering the scenario where

$$\mu_- < \mu < \mu_+. \tag{14}$$

Fast timescale
We consider $T=\tau/\epsilon$. The governing equations on this fast timescale are

$$\frac{dv}{dT} = f(u,v), \quad \frac{d}{dT}(u+\gamma v) = 0, \tag{15}$$

so that we have rapid relaxation to $f(u,v)=0$ (to leading order) with $u+\gamma v = \text{const}$.
Slow timescale
On this timescale, we have $f(u,v)=0$ so that $v=g(u)$, together with

$$\frac{d}{d\tau}(u+\gamma v) = \mu - u. \tag{16}$$

On this timescale the trajectory moves along the nullcline $v=g(u)$.
We thus obtain periodic solutions when the equilibrium point μ is such that $\mu_- < \mu < \mu_+$, and the system moves between fast and slow dynamics. See figure 12.

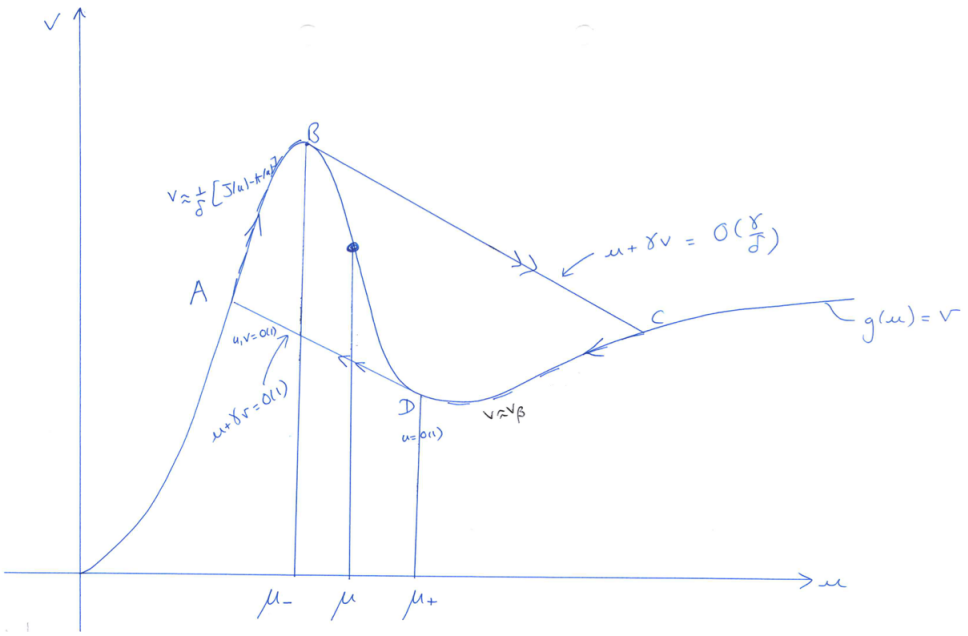

Figure 12: Fast-slow dynamics.

We can consider the behaviour of u, *i.e.* non-dimensional cytosolic calcium, as a function of time. Here for example we consider the period of the oscillation. We refer again to figure 12.

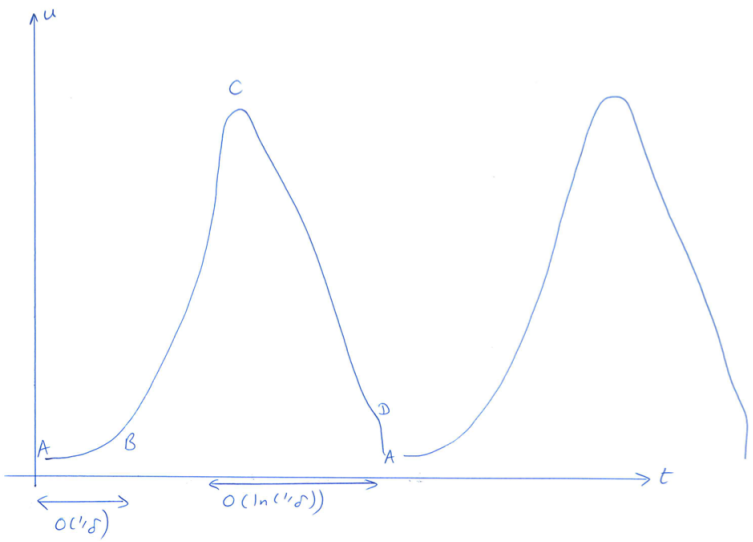

Figure 13: Oscillations for u.

Note that the labels A-D on figure 12 do not correspond to those on figure 8 etc.
On DA and BC the timescales are $O(\epsilon)$ as we are in the fast dynamics regime.
On CD, we roughly have that $g \approx v_\beta$, so that $v \approx v_\beta$ (and we can neglect the derivative of v with respect to τ), and hence

$$\frac{du}{d\tau} \approx \mu - u. \tag{17}$$

Thus

$$u \approx \mu - (\mu - u_C)\exp(-\tau + \tau_C), \tag{18}$$

where we adopt the notation that u_C etc refers to the value of u at the point C.
Now on CB $u + \gamma v = \text{const}$. Hence we have that $u_B + \gamma v_B = u_C + \gamma v_C$. At B, $u_B = \mu_- \ll v_B = O(1/\delta)$. Thus we have that $u + \gamma v = O(\gamma/\delta)$ on BC. At C, $v_C \approx \beta = O(1)$, so that on BC u jumps up to $O(1/\delta)$ while v jumps down to $O(1)$. At D we have that u jumps down to $O(1)$. From (18), we can show that the timescale on CD over which u drops from $O(1/\delta)$ to $O(1)$ is

$$t = O\left(\ln \frac{1}{\delta}\right). \tag{19}$$

Since at D we have that both u and v are $O(1)$, then on AD we must have that $u + \gamma v = O(1)$. Now, on AB, $v = g(u) \approx \frac{1}{\delta}(J(u) - K(u))$. This implies that

$$\frac{du}{d\tau} \approx \frac{\mu - u}{1 + \frac{\gamma}{\delta}(J'(u) - K'(u)} = \delta \frac{\mu - u}{\delta + \gamma(J'(u) - K'(u))} = O(\delta). \tag{20}$$

Hence the timescale of the trajectory along AB (for $u = O(1)$) is $O(1/\delta)$.

Since $\delta \ll 1$, the dominant timescale of the period is the time spent on AB. Hence, to leading order, the period is

$$\int_A^B d\tau = \int_{u_A}^{u_B} \frac{du}{du/d\tau} = \frac{1}{\delta}\int_{u_A}^{u_B} du \frac{\delta + \gamma(J'(u) - K'(u)}{\mu - u}. \tag{21}$$

Now $v = g(u)$ is determined from $f(u, v) = 0$. However, $f(u, v)$ does not depend on μ, and hence $v = g(u)$ does not depend on μ. Furthermore, u at point D is determined from the solution of $g'(\mu_+) = -1/\gamma$, so that u_D is independent of μ (a similar argument applies for u_B). At D we also have that $v = g(u)$ which implies that $u + \gamma v$ is independent of μ. Since at A, $v_A = g(u_A)$, we also have that u_A is independent of μ. Hence, on AB, we have that

$$\frac{\partial}{\partial \mu}\left(\int_A^B d\tau\right) = -\int_{u_A}^{u_B} du \frac{\gamma(J'(u) - K'(u))}{\delta[\mu - u]^2} < 0. \tag{22}$$

Now

$$v = g(u) \approx \frac{1}{\delta}(J(u) - K(u)) \tag{23}$$

on AB thus the numerator in (22) is $1 + \gamma g'(u)$ and for $u_A, u_B < \mu$ we have $g'(u) \geq 0$. Hence the numerator is positive, and $\partial P/\partial \mu < 0$, so that the period decreases as μ increases. The amplitude of the oscillation is approximated by u_C, which is independent on μ.
Putting all this together, we the solution of u as a function of t in depicted in figure 13. The oscillations are spiky, with an asymmetrical shape.

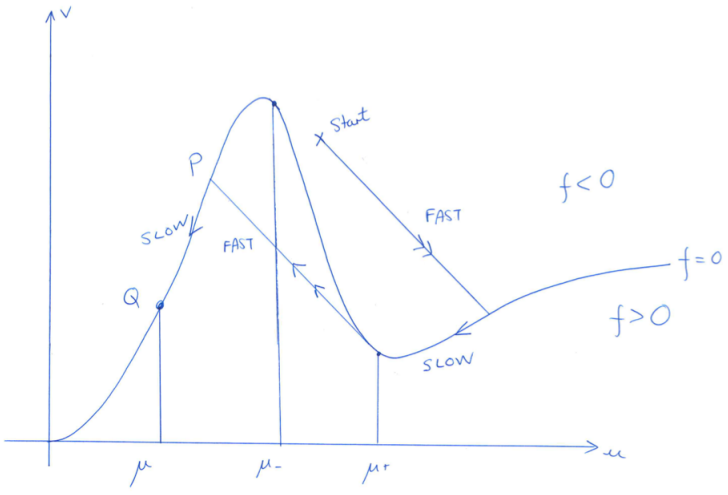

Figure 14: The phase plane corresponding to $\mu < \mu_-$.

Now suppose we consider the phase plane dynamics when

- $\mu < \mu_-$

This is shown in figure 14. We see that the system exhibits excitable dynamics, with large excursions in the phase plane. Eventually the trajectory returns to its steady state, and u decreases on PQ since

$$\frac{d}{d\tau}(u + \gamma v) = \mu - u < 0. \tag{24}$$

Note that the perturbation must be large enough to initiate the phase-plane excursion.
The case with $\mu > \mu_+$ has analogous dynamics.

3.2 Calcium Waves

Ca^{2+} waves can propagate within cells at speeds of 10-100 microns per second, especially in large cells such as oocytes (fertilised eggs) where periodic wavetrains are observed; in frog oocytes, spiral waves of calcium are also seen.

We consider the two pool model in a cell sufficiently large that we do not have a spatially homogeneous distribution of Ca^{2+}, so that diffusion is important. In contrast, the calcium stores are assumed to be no larger than normal cells and hence calcium is taken to be spatially homogeneous in these compartments.

Thus, for a one dimensional wave, with the same non-dimensonalisation as above, we have

$$u_t + \gamma v_t = \mu - u + \nu u_{xx}, \quad \epsilon v_t = f(u, v),$$

with

$$\nu = D/[kL^2],$$

where D is the diffusion coefficient and L is the diffusive lengthscale.

Below, if $\nu \ll \epsilon$ we have that diffusion is negligible and can be neglected; given we observe spatially heterogeneous waves (in oocytes at least), we are not in this parameter regime. If $\nu \gg \epsilon$ we have $u_{xx} = 0$ at leading order and again we do not a wave behaviour. Thus we require $\nu \sim \epsilon$ and we take the diffusive lengthscale to be such that $\nu = \epsilon$.

For parameter values

$$D \sim 10\mu\text{m}^2\text{s}^{-1}, \quad k = 10\text{s}^{-1}, \quad \epsilon = 0.04,$$

we have $L \sim 5\mu$m, which is reasonable.

We seek travelling wave solutions and set $u = u(\zeta),\ v = v(\zeta)$ where $\zeta = x + st$, where $s > 0$ is the travelling wavespeed, to obtain:

$$s(\dot{u} + \gamma\dot{v}) = \mu - u + \epsilon\ddot{u}, \qquad \epsilon s\dot{v} = f(u, v),$$

where "dot" denotes $d/d\zeta$.

Diffusion entails that the large transitions in cytosolic calcium will occur at different values compared to the spatially homogeneous analogue. We consider a path in (u, v) space of the form given in figure 15, though we do not fix the values of $u,\ v$ at the points $A,\ B,\ C,\ D$ *a priori*.

Figure 15: The phase plane.

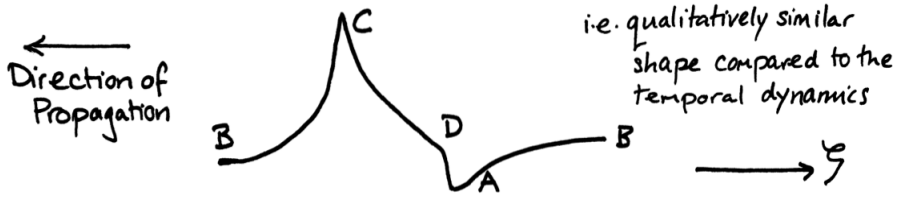

Figure 16: The trajectory.

We expect the travelling wave to be of the form in figure 16.
On CD and AB we have slow dynamics, which is approximated by taking $\epsilon = 0$ above to yield the leading order equations

$$f(u,v) = 0, \quad s\left(1 + \gamma \frac{dg}{du}(u)\right)\dot{u} = \mu - u.$$

On BC we have fast dynamics and thus we write $\zeta = \epsilon X$ to give the equations

$$s(u' + \gamma v') = u'', \tag{25}$$

$$v' = \frac{1}{s} f(u,v), \tag{26}$$

where prime denotes d/dX. Integrating on BC gives

$$u' = s(u + \gamma v) - J_{BC} \tag{27}$$

where J_{BC} is a constant of integration.

On BC, matching the fast and slow dynamics solutions, at the point B and also at the point C, gives

$$J_{BC} = s(u_B + \gamma v_B) = s(u_C + \gamma v_C), \quad \text{with } \; f(u_B, v_B) = f(u_C, v_C) = 0. \tag{28}$$

This is because on BC we have a second order autonomous set of differential equations, i.e. (26) and (27), that match into the slow dynamics as $X \to \pm\infty$. Gradients in the slow dynamical regime are much smaller than in the fast dynamical regime, and hence in the asymptotic limit we must have the fast dynamical system gradients tending to zero (so that $u',\ v' \to 0$ as $X \to \infty$). The values of $u,\ v$ therefore tend to equilibrium points of the fast dynamical system giving the constraints (28) on inspection of (26), (27).

Writing $U = u - u_B$, $V = v - v_B$, $F(U,V) = f(u,v)$ we have

$$U' = s(U + \gamma V), \quad V' = \frac{1}{s} F(U,V), \qquad \frac{dV}{dU} = \frac{1}{s^2} \frac{F(U,V)}{U + \gamma V}.$$

Phase Plane

We require a phase plane connection between the saddle (1) and saddle (3). This requires the unstable manifold (denoted $*$) to connect with the stable manifold (denoted $**$); see figure 17.

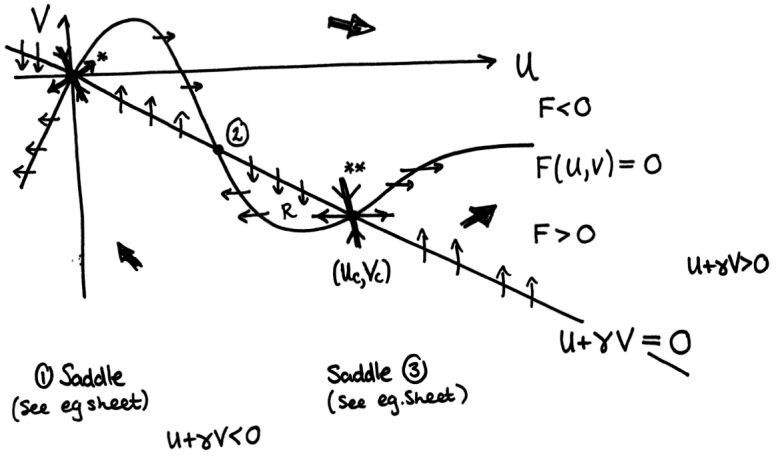

Figure 17: Connections between saddles in the phase plane.

We consider the cases s large, and s small (figure 18).

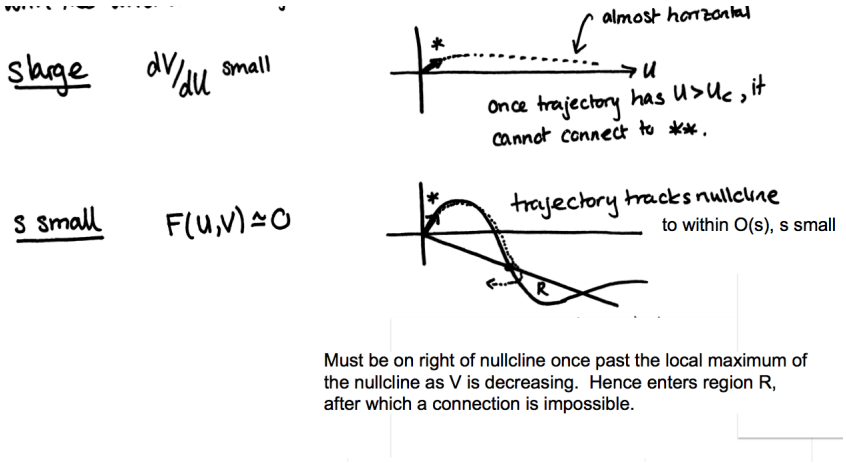

Figure 18: Trajectories for large and small s.

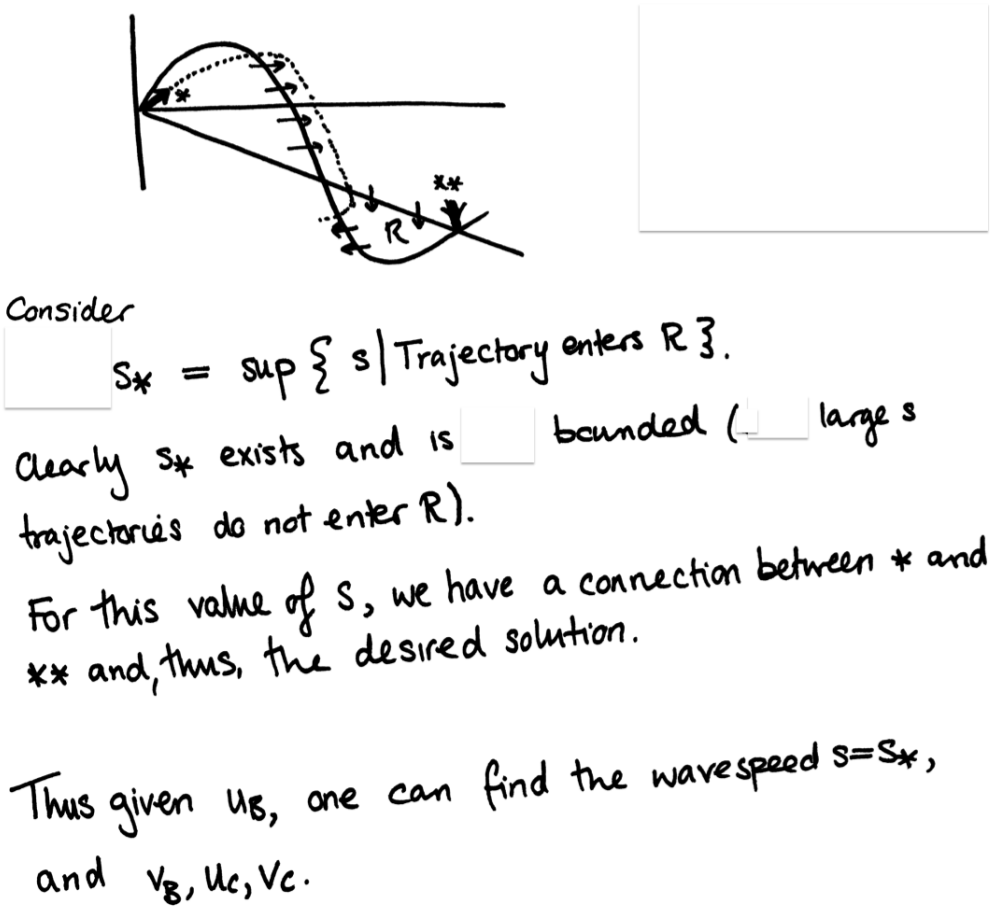

Figure 19: Determining the wave speed.

On DA Again we have fast dynamics. Analogously to BC we write $\zeta - \zeta_1 = \epsilon X_1$, where ζ_1 is displaces the DA front from the BC front along the travelling wave. This gives the equations

$$u' = s(u + \gamma v) - J_{DA} \tag{29}$$

where prime denotes d/dX_1 and

$$J_{DA} = s(u_D + \gamma v_D) = s(u_A + \gamma v_A), \quad \text{with} \quad f(u_D, v_D) = f(u_A, v_A) = 0. \tag{30}$$

Suppose u_D is fixed. Then $v_D,\ u_A,\ v_A$ can be found. Writing $U = u - u_A$, $V = v - v_A$, $F(U,V) = f(u,v)$ we once more have

$$U' = s(U + \gamma V), \quad V' = \frac{1}{s}F(U,V), \qquad \frac{dV}{dU} = \frac{1}{s^2}\frac{F(U,V)}{U + \gamma V}.$$

We can find the travelling wavespeed by requiring a phase plane connection, as before. However, the resulting wavespeed, denoted s_*^D, need not be the same as s_*, and thus there is no travelling wave solution. Requiring $s_*^D = s_*$ constrains u_D. Thus given u_B, u_D and consequently $v_D,\ u_A,\ v_A$

are determined.

In summary, there is a one parameter family of travelling wave solutions of different speeds, obtained by varying u_B.

Finally, note that the wavelength can be found by integrating

$$s\left(1+\gamma\frac{dg}{du}(u)\right)\dot{u}=\mu-u$$

on CD and AB.